Available online at www.sciencedirect.com
SCIENCE DIRECT®
Journal of Crystal Growth 271 (2004) 13–21
JOURNAL OF CRYSTAL GROWTH
www.elsevier.com/locate/jcrysgro

Predicting GaAs surface shapes during MBE regrowth on patterned substrates

A. Ballestad[a,*], T. Tiedje[a,b], J.H. Schmid[a], B.J. Ruck[c], M. Adamcyk[d]

[a]*Department of Physics and Astronomy, University of British Columbia, 443-2355 East Mall, Vancouver, Canada, BC V6T 1Z1*
[b]*Department of Electrical and Computer Engineering, University of British Columbia, Vancouver, Canada, BC V6T 1Z4*
[c]*School of Chemical and Physical Sciences, Victoria University of Wellington, New Zealand*
[d]*Optical Communication Products Inc., Bloomfield, CO, USA*

Received 2 March 2004; accepted 20 July 2004
Communicated by M. Uwaha
Available online 13 September 2004

Abstract

We have developed a continuum model based on two coupled differential equations that explains the complex surface shapes observed in epitaxial regrowth on micron scale gratings. This model describes the dependence of the surface morphology on film thickness and growth temperature in terms of a few simple atomic scale processes including adatom diffusion, step-edge attachment and detachment, and a net downhill migration of surface adatoms. The continuum model reduces to the linear part of the Kardar–Parisi–Zhang equation with a flux dependent smoothing coefficient in the long wavelength limit.

PACS: 81.10.Aj; 81.15.Aa; 68.55.−a

Keywords: A1. Computer simulation; A1. Crystal morphology; A1. Growth models; A1. Morphological stability; A3. Molecular beam epitaxy; B2. Semiconducting gallium arsenide

1. Introduction

The problem of the time evolution of the shape of crystal surfaces has a long history dating back to Mullins and Herring who considered relaxation during annealing above the roughening temperature [1]. More recently, shape relaxation below the roughening temperature has been studied extensively [2–4]. Below the roughening temperature the problem is complicated by the need to keep track of the dynamics of atomic steps and the fact that the surface free energy of crystal facets is singular. Biasiol et al. [5] have extended the theory of shape relaxation below the roughening temperature to

*Corresponding author. Tel.: +1-604-822-5425; fax: +1-604-822-4750
E-mail address: anders@physics.ubc.ca (A. Ballestad).

0022-0248/$ - see front matter © 2004 Elsevier B.V. All rights reserved.
doi:10.1016/j.jcrysgro.2004.07.047

include the effects of atom deposition, and use this theory to explain the self limiting V-grooves observed in organo-metallic chemical vapor deposition growth on corrugated GaAs substrates. In this paper we present a new continuum model which we use to interpret measurements of the shape of corrugated (0 0 1) GaAs surfaces under growth conditions which do not produce faceting. Facets are not present in our experiments due to atomic scale roughness associated with atom deposition in the island growth mode, and the fact that the surface topography is sufficiently weak that the surface slope does not reach the low-energy [1 1 1] facets. We show that this model reproduces the surface morphology that develops during molecular beam epitaxy (MBE) regrowth on 1D surface gratings.

2. Conventional modeling of weak surface texture

The evolution of long wavelength, low amplitude, surface structures during GaAs homoepitaxy can be described by the Kardar–Parisi–Zhang (KPZ) equation [6,7]: $\partial_t h = \nu\nabla^2 h + \frac{\lambda}{2}(\nabla h)^2 + F + \eta(x,t)$. The coefficients in this equation are constants characterizing the microscopic atomic processes. The source term $\eta(x,t)$ simulates the random arrival of atoms at an average rate F. According to this equation, a textured starting surface will develop parabolic mounds that smooth with time separated by V-shaped valleys. Recent steady state growth experiments [8] have shown that the KPZ equation provides a quantitative description of the power spectral density of the surface morphology of epitaxially grown GaAs layers for surfaces with low amplitude, long wavelength, characterized by local slopes $\lesssim 3^\circ$. These experiments are consistent with the leading term $\nabla^2 h$ in the KPZ equation and not with the leading term $\nabla^4 h$ in the so-called MBE equation [9,10]. The agreement with this simple KPZ continuum model suggests that the anomalous effects associated with the singular free energy of crystal facets are not important for the growth conditions in question [4]. This is likely a consequence of the fact that under our growth conditions the surface is above the roughening temperature [11].

In the case of GaAs MBE growth with no re-evaporation, the linear term $\nabla^2 h$ in the KPZ equation means that there must be a net downhill flux of adatoms proportional to the negative surface slope: $\mathbf{j} \sim -\nabla h$ (so that $\partial_t h \sim -\nabla\cdot\mathbf{j} \sim \nabla^2 h$) [1]. The simplest explanation for such a downhill current is that it is due to a negative Ehrlich–Schwoebel (ES) effect, namely a step edge potential barrier that favors downhill migration of adatoms. Experiments in metal epitaxy have shown positive ES barriers [12], however, the situation for III–V semiconductor surfaces is much more complex with surface reconstructions, complex step edge geometries and a two component (Ga,As) surface [13–15]. Although the simple ball model [1] with Lennard–-Jones type potentials would suggest that the ES barrier is always positive, more realistic calculations show that the situation for real materials is not always this clear, that for certain step orientations "the potential is maximum at the center of the terrace rather than on the terrace edge", even for elemental metals (see pp. 94 and 95 in Ref. [1]). In an influential paper, Johnson et al. [16] proposed that the mounds observed in GaAs growth on thermally de-oxidized (0 0 1) surfaces were caused by positive ES barriers, which lead to unstable growth and mounding [16,17]. In later work, the mounds observed in GaAs buffer layers were found to be associated with the smoothing of the surface roughness created during the thermal oxide desorption from the starting surface and the mounds were observed to smooth with time [7,8,18,19], consistent with a downhill flux of adatoms. Simulations based on the stable KPZ equation supported these observations [7,8].

A net downhill flux of adatoms could also occur in the presence of positive ES barriers if other growth phenomena are present which counteract the effect of the ES barriers. Two such possibilities that have been discussed in the literature arise from the excess energy associated with an atom incident from the vapor. These are known as downhill funneling [20] and step edge knockout [1]. In downhill funneling an adatom deposited near a step edge will have excess energy that

enables it to diffuse to a low-potential site close to the original impact point. In the case of step edge knockout, an energetic adatom deposited just above a step edge can push the step edge atom aside and insert behind the step edge. These processes all create a downhill flux that could in principle overwhelm the effect of a positive ES barrier. Orme et al. [17] show how these countering effects can lead to a "magic slope", for which the adatom current is zero. This was then used to explain the slope selection observed experimentally [17], however, again, later experimental results indicate no such "magic slope" [7,8,18,19], and the countering current mechanisms are not necessary in order to describe the surface shape evolution. It remains an unresolved issue, therefore, whether the stable, downhill adatom current term is caused by a negative ES barrier or the combined effect of a positive barrier along with a stronger counteracting, stabilizing effect.

The nonlinear term in KPZ is associated with growth along the outward normal, as in chemical vapor deposition. In this case, which is not applicable in MBE, λ should be equal to the growth rate F. However, the value for λ needed to simulate the experimental results is almost two orders of magnitude larger than F [8]. This raises the question as to the physical origin of the nonlinear term in MBE growth. The KPZ nonlinearity is non-conservative, whereas, MBE growth is conservative with a growth rate that is independent of the surface shape. In practice, for the low surface slopes where KPZ is applicable, the change in growth rate associated with the nonlinear term is very small. Although the KPZ nonlinearity gives a good approximation to the surface shape its physical origin is obscure in the case of MBE growth. One would prefer to have a model that can be derived from underlying physical phenomena.

In addition, the KPZ description with constant coefficients is not consistent with experiments which show that the smoothing rate depends on the growth rate. For example, in Fig. 1 we show the scattered light intensity from a GaAs surface during an interruption in growth on a randomly textured substrate. The intensity of scattered light is proportional to the power spectral density of the surface topography at a spatial frequency q determined by the optical wavelength and geometrical factors [8]. In this case $q = 41\,\mu m^{-1}$, corresponding to a lateral surface length-scale of about 150 nm. For low amplitude surface textures, in the KPZ model the surface should smooth exponentially with a characteristic rate given by vq^2 where q is the spatial frequency of the surface roughness [1]. As shown in the inset of Fig. 1, the smoothing rate responds immediately to changes in the growth flux; it is faster during deposition and slower during annealing, suggesting that v is flux dependent. This continued smoothing of the surface in the absence of an atom flux indicates that the physical mechanisms at play on the surface favor a net downhill migration of surface adatoms, even when the flux of atoms is turned off. This suggests that if there are two competing mechanisms including a positive ES barrier that the stabilizing mechanism that creates the downhill flow is not associated with energetic adatoms deposited from the vapor such as step edge knockout or downhill funneling.

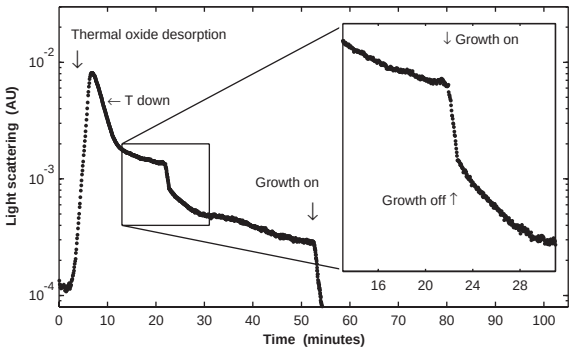

Fig. 1. Light scattering during growth corresponding to surface power spectral density at 41 μm^{-1} showing the effect of atom deposition on the smoothing rate. The sample roughens during a temperature ramp to remove the surface oxide at about 5 min in the figure, which is followed by relatively fast smoothing during a high temperature (620 °C) anneal for about 7 min, and then slower smoothing during annealing at growth temperature (550 °C)

To summarize, the KPZ equation provides an accurate description of the surface morphology under certain restricted conditions (constant growth rate, low surface slope and long wavelength surface structures). In addition, the physical

origin of the nonlinearity in KPZ is unclear in the case of MBE growth. In the rest of this paper we develop a new continuum model based on a few simple physical processes that describes the surface morphology over a broader range of conditions than the KPZ equation and we compare this model with experimental data.

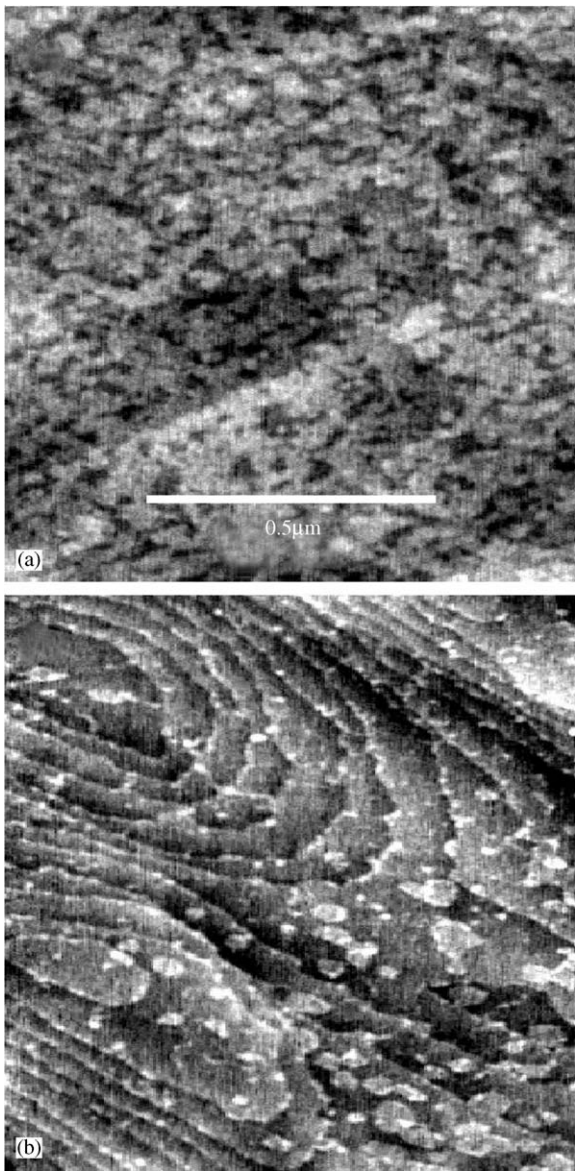

Fig. 2. AFM images of (a) a sample quenched (fast cooled) after 69 min of growth at 600 °C and (b) a sample annealed for 15 min at growth temperature 595 °C after 40 min of growth.

To illustrate the physical processes involved in the epitaxial growth process and to motivate the new model we compare atomic force microscope (AFM) images of a growth surface which is fast cooled after growth is terminated (quenched) with one that has been annealed (see Figs. 2a and 2b). In this figure and in Fig. 1, the As_2/Ga flux ration was 10:1. The quenched sample (a) is covered with small islands, whereas the annealed sample (b) has broad terraces with few islands. The small islands must coalesce into the step edges during annealing. The kinetic barrier to the adatom coalescence into the step edges, causes the growth process to be non-local in space and time. This means that the growth rate at one location will be affected by the morphology at another location in contrast to KPZ, for which the growth rate only depends on the local surface slope and curvature. This is a problem not only for KPZ but also for alternative growth equations such as the MBE Equation [1]. Physically, a high density of steps at one location that absorb adatoms will affect the adatom density and hence the growth rate at another nearby location.

3. Coupled growth equation model

The growth phenomena discussed above can be explained in a natural way if we extend the growth model to include the adatom dynamics explicitly with two 1D coupled growth equations (CGE) [21]:

$$\partial_t n + \nabla \cdot \mathbf{j} = F - a_{\parallel}^{-1}\partial_t(a_{\perp}^{-1}h), \tag{1a}$$

$$\partial_t(a_{\perp}^{-1}h) = \beta D n^2 + \beta D n S - a_{\parallel}\kappa S. \tag{1b}$$

Eq. (1a) is a continuity equation for the adatom density n (in units of nm^{-1}) with source and sink terms, while Eq. (1a) describes the time dependence of the surface height h (in nm), which depends on the dimer nucleation rate and the net adatom attachment rate at steps. The constants are defined as follows: F is the deposition rate from the vapor (in $nm^{-1}\ s^{-1}$), D the adatom diffusion coefficient (in $nm^2\ s^{-1}$), S the density of steps (in nm^{-1}), κ the rate of thermal detachment of atoms from step edges into the adatom phase (in s^{-1}),

and β is the incorporation coefficient for an adatom to a step edge or to another adatom. The lattice parameters are $a_{\parallel}$ (in-plane) and $a_{\perp}$ in the growth direction. An adatom is defined as a diffusing unit on the surface, which could be a Ga atom or a Ga-As complex. Eqs. (1a) and (1b) are continuum equations in the sense that the variables, namely the surface height, adatom density and step density are macroscopic quantities averaged over a number of atomic units. In Eq. (1b), any adatom that attaches to a step edge is assumed to have incorporated into the film. We also define:

$$\mathbf{j} = -D(a_{\perp}^{-1}\zeta n\nabla h + \nabla n), \tag{2a}$$

$$S = \sqrt{S_0^2 + (a_{\perp}^{-1}\nabla h)^2}, \tag{2b}$$

where in Eq. (2a), $\mathbf{j}$ is the surface current of adatoms and ζ is a proportionality constant which describes the net directional drift of adatoms. A positive value for ζ gives a net downhill adatom current, consistent with the surface smoothing that is observed experimentally for GaAs (0 0 1) [8,18,19]. At this point the form for the surface current in Eq. (2a) can be regarded as a hypothesis, motivated by the success of the second order linear term in the KPZ equation in fitting the GaAs surface morphology in the limit of low surface slopes [7]. The second term in Eq. (2a) represents adatom diffusion.

Eq. (2b), is a physically plausible expression for the dependence of the rms step density on the surface slope. In this equation, S_0 is the random step density on a flat surface due to growth related phenomena such as island nucleation and thermally induced disorder. This step density will depend on temperature, growth rate, arsenic flux and on time, if the growth rate is not constant (see Fig. 2a and b) [22]. If the random step density is not too large, one can define a random local slope associated with the local configuration of the steps. In the presence of a macroscopic topography the random local slope associated with S_0 adds to the macroscopic slope ∇h. If the two slopes are uncorrelated then the rms step density is given by Eq. (2b). In general there may be correlations between S_0 and ∇h. Nevertheless, one might expect this expression for the step density to be relatively insensitive to correlations, as it has the correct limiting behavior for large and small surface slopes. Therefore one could also regard Eq. (2b) as a convenient interpolation formula.

In the limit that $\nabla h < S_0$ there will be numerous up and down steps (i.e. small islands) between successive net upward (or net downward) steps associated with the macroscopic surface slope. The net downward flux associated with the step edge ES barriers or other mechanisms which drive the flow of adatoms downhill will depend on the macroscopic average surface slope. For example, a monolayer island located on a terrace on a vicinal surface, will not cause a net macroscopic downhill flux of adatoms, even in the presence of ES barriers as the down flow on one side of the island will balance the down flow in the opposite direction on the other side. For this reason the adatom current in Eq. (2a) is proportional to the macroscopic surface slope ∇h.

The simple picture of a surface consisting of flat terraces separated by atomic steps, can be expected to provide a good description of the surface as long as the surface slope does not reach the next low index crystal planes, namely (1 1 0) and (1 1 1). These planes are 45° and 54.7° from the surface normal, and are beyond the range of surface slopes that we have explored experimentally ($\lesssim 30°$).

For low amplitudes and long wavelength ($\nabla h < S_0$), the adatom density will be nearly constant as a function of position and time, and approximately equal to $n_0 = (F + \kappa S_0)/\beta D S_0$. In this case, Eqs. (1a) and (1b) reduce to,

$$\frac{\partial h}{\partial t} = \frac{\zeta}{\beta}\left(\frac{F}{S_0} + \kappa\right)\nabla^2 h + F. \tag{3}$$

This reproduces the linear part of the KPZ equation and shows explicitly the dependence of the linear smoothing coefficient ν on the deposition rate and the downhill drift parameter ζ. In addition, it shows that in the absence of growth ($F = 0$) the linear smoothing term is independent of the background step density S_0. This agrees with the light scattering data in Fig. 1, which shows that the smoothing rate is relatively constant during a growth interruption even though the AFM images in Fig. 2 indicate that the step

density drops dramatically during annealing. Extending Eq. (3) to higher order, one finds nonlinear terms with higher order spatial derivatives. We speculate that the higher order nonlinear terms can be approximated by the KPZ nonlinearity over a limited spatial frequency range if the surface topography is not too large.

4. Patterned surfaces: film thickness evolution

Growth on substrates with larger amplitude surface slopes, up to $\sim 30^{\circ}$, show complex surface shapes before evolving into parabolic mounds, as shown in Fig. 3(a). At intermediate times, the valleys are V-shaped with concave rather than convex sidewalls and distinct shoulders near the top of the sidewalls. Note the absence of (0 0 1) facets which are predicted theoretically for annealing below the roughening temperature in the absence of deposition [4]. Eqs. (1) and (2) an be solved in seconds with a finite difference scheme and a coupled differential-algebraic system solver, and a 1D solution is shown in Fig. 3(b) with parameters adjusted to match the experimental data in Fig. 3(a) (see Table. 1 for parameters). The agreement with the experimental surface shapes is striking. In particular, the model reproduces the inverted ''Gothic window'' shape of the valley for the 600 nm growth and the KPZ-like cusps in the 2600 nm growth where the grating amplitude has reduced significantly.

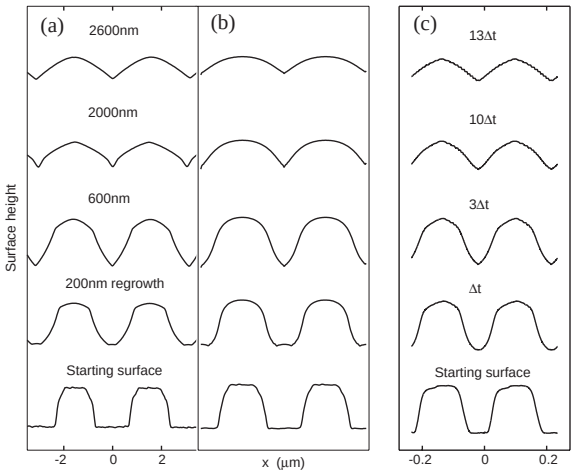

Fig. 3. Film thickness dependence: (a) AFM scan lines for regrowth on 100 nm deep gratings oriented perpendicular to the [110] direction (substrate temperature was 580°C, $F = 1$ML/s and the As_2/Ga pressure was 3:1); (b) Scan lines from CGE calculation; (c) Scan lines from 2D kMC simulation of 10 nm high grating structure, where one Δt equals 5.6 ML of growth. All offsets arbitrary.

A continuum model cannot include the microscopic details of the atomic scale phenomena, such as the geometrical configuration of the step edges. We therefore compare the continuum model described by Eqs. (1) and (2) with a kinetic Monte Carlo (kMC) simulation, which includes the same physical processes that are included in the Eqs. (1). We use a 2D, cubic grid, one-component, restricted solid-on-solid (SOS) model, with nearest-neighbor interaction. Each atom bonds to the surface with an activation energy $E_{act} = E_{sub} + mE_{lat}$, where m is the number of lateral neighbors [23]. It should be noted that in these simulations, a negative ES barrier was used, as described in Section 2. The kMC simulations produce a random step distribution automatically due to the statistical nature of the model. In kMC, the

Table 1
Parameter table for CGE calculations.

Figure	F (ML/s)	T (°C)	$D/10^5$ (nm^2/s)	κ (1/s)	S_0 (1/nm)	$\beta/10^{-4}$	$\zeta/10^{-3}$
3 (b) ($\perp$ [1 1 0])	1.0	580	2.5	4.3	0.07	3.3	1.4
4 (b) ($\perp$ [1 $\bar{1}$ 0])	0.8	420	0.04	0.004	0.49	6.6	1.5
		500	0.4	0.2	0.38	1.6	1.4
		550	1.3	1.4	0.19	0.4	1.2
		610	4.6	12	0.03	13	1.1

binding energy for an atom at a step edge depends on how many neighbors it has ($\sim mE_{\mathrm{lat}}$), whereas in the CGE continuum model a single average value is used for the step edge binding energy. SOS simulations of MBE growth by kMC are limited by available computing power to small scale structures, and become intractable for realistic, high temperature growth scenarios where 2D systems have sides up to microns and growth times on the order of hours. In Fig. 3(c), we show a kMC simulation for a surface grating that is somewhat smaller than the experimental structures. The simulated grating profiles in Fig. 3(c) were obtained by projecting 2D kMC simulations onto a line at each time point by taking the average elevation perpendicular to the scan line. In this simulation, $E_{\mathrm{sub}} = 1.25$ eV, $E_{\mathrm{lat}} = 0.35$ eV and an ES step-edge barrier of $E_{\mathrm{ES}} = -0.05$ eV was used for the downhill drift mechanism. The agreement with the experimental shapes is excellent, reproducing all of the main features, except they are on a smaller size scale. The substrate and lateral binding energies are similar to values reported earlier in the interpretation of RHEED data [24,25] and compatible with the fitting parameters found in the continuum model. It is plausible that similar shapes could be obtained for the larger size scales relevant to the experiments by scaling the parameters appropriately. In the case of the CGE model(Eqs. (1) and (2)) we find that the parameters can indeed be scaled to yield similar surface shapes at different length scales [26].

5. Patterned surfaces: temperature evolution

In Fig. 4(a), we show the dependence of the surface topography on growth temperature, for a fixed layer thickness together with Fig. 4(b) the simulated surface topography using Eqns. (1) and (2) parameters as outlined in Table. 1. The experimental data is obtained from growths on 100 nm deep gratings oriented perpendicular to $[1\,\bar{1}\,0]$. This is the faster diffusion direction in this material system [8], and depends on the As_2/Ga ratio during growth, which was equal to three for the data shown in Figs. 3 and 4. This observation

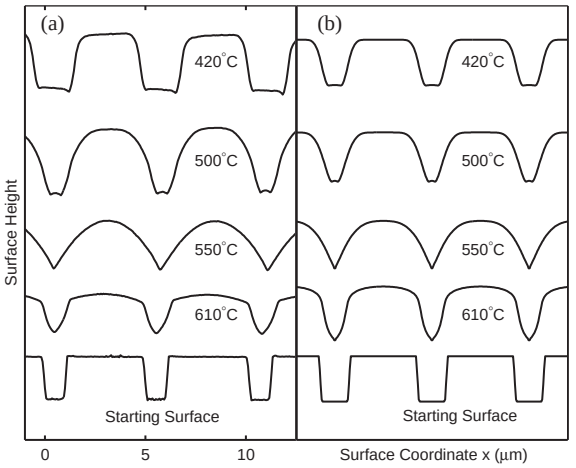

Fig. 4. Growth temperature dependence: (a) AFM scan lines for regrowth on 100 nm deep gratings oriented perpendicular to the $[1\bar{1}0]$ direction; (b) CGE calculation. The grating pitch is 5 μm. All growths are 1 h at 0.8 ML/s and the As_2/Ga pressure was 3:1. All offsets arbitrary.

is consistent with the values used for the downhill drift parameter in our calculations, where the best fits were obtained using a larger ζ when the gratings were oriented perpendicular to $[1\,\bar{1}\,0]$ (Fig. 4(b)) than for gratings perpendicular to the $[1\,1\,0]$ direction (Fig. 3(b)). The diffusion constant D, however, was considered isotropic in all calculations in this paper. There is some uncontrolled variation in the pitch and depth of the gratings in the experimental data in Fig. 4(a). Nevertheless, the CGE model reproduces the main features in the temperature dependent data, namely the small secondary mound in the valley at 420 °C and 500 °C, the KPZ-like cusp at 550 °C and the inverse Gothic window shape for the valleys at 610 °C. The shoulders at the edges of the ridges at 610 °C are also reproduced by the model, although they are not as sharp as in the experimental data.

The parameters used in these calculations are based on the same energies used in the kMC simulations in Fig. 3(c). The diffusion constant is related to the substrate binding energy through the expression $D = (2kT/h)\exp(-E_{\mathrm{sub}}/kT)$. The step edge detachment rate is calculated from $\kappa = D\exp(-\hat{m}E_{\mathrm{lat}}/kT)$, where $\hat{m}$ is an average number of neighbors for atoms at a step edge which we set

equal to 2.5. The declining value of S_0 with temperature is reasonable under growth conditions; one might also expect ζ to decrease weakly with temperature. Satisfactory fits to the data were also obtained with a larger activation energy for D (1.8 eV rather than 1.25 eV) together with a smaller prefactor and somewhat different (yet still physically reasonable) temperature dependences for the other parameters. Experimental and theoretical work suggests that the activation energy for D is in the 1.5–2.0 eV range [24,25,27,28].

In a recent publication, Kan et al. [29] find that the peak-to-valley amplitude of patterned GaAs surfaces increases during the initial stages of regrowth before declining. This effect is also present in the CGE model. For example in Fig. 3, both the data (panel a) and the CGE calculations (panel b) show that the surface peak-to-peak amplitude has increased after 200 and 600 nm film growth, but has decreased again at longer growth times. Fig. 4 shows the same effect, where both the data (panel a) and the CGE calculations (panel b) show an increase in the surface peak-to-valley amplitude. It is interesting to note that a stable model like the one described in this paper, with a net downhill drift of adatoms still can create a seeming instability like the peak-to-valley amplitude overshoot.

6. Conclusions

We have shown that the complex surface shapes which develop during epitaxial regrowth on patterned (0 0 1) GaAs substrates, can be explained by the dynamics of the deposited adatoms, including step edge attachment and detachment, adatom diffusion, and a stable, downhill adatom drift. Although we attribute the downhill drift to a negative ES barrier we cannot rule out the possibility that this effect is caused by some other mechanism. This analysis is specific to GaAs, but the concepts are generic and should be applicable to other systems.

Acknowledgements

We thank K. L. Kavanagh and D. D. Vvedensky for helpful suggestions.

References

[1] A. Pimpinelli, J. Villain, Physics of Crystal Growth, Cambridge Univ. Press, Cambridge, 1998.
[2] P.M. Duxbury, T.J. Pence (Eds.), Dynamics of Crystal Surface and Interfaces, Plenum Press, NY, 1997.
[3] J. Erlebacher, M.J. Aziz, E. Chason, M.B. Sinclair, J.A. Floro, Phys. Rev. Lett. 84 (2000) 5800.
[4] V.B. Shenoy, A. Ramasubramaniam, L.B. Freund, Surf. Sci. 529 (2003) 365.
[5] G. Biasiol, A. Gustafson, K. Leifer, E. Kapon, Phys. Rev. B. 65 (2002) 205306.
[6] M. Kardar, G. Parisi, Y.-C. Zhang, Phys. Rev. Lett. 56 (1986) 889.
[7] A. Ballestad, B.J. Ruck, M. Adamcyk, T. Pinnington, T. Tiedje, Phys. Rev. Lett. 86 (2001) 2377.
[8] A. Ballestad, B.J. Ruck, J.H. Schmid, M. Adamcyk, E. Nodwell, C. Nicoll, T. Tiedje, Phys. Rev. B 65 (2002) 205302.
[9] T. Sun, H. Guo, M. Grant, Phys. Rev. A 40 (1989) 6763.
[10] Z.-W. Lai, S. Das Sarma, Phys. Rev. Lett. 66 (1991) 2348.
[11] Z. Ding, D.W. Bullock, P.M. Thibado, V.P. LaBella, K. Mullen, Phys. Rev. Lett. 90 (2003) 216109.
[12] T. Michely, M. Kalff, G. Comsa, M. Strobel, K.H. Heinig, J. Phys. Cond. Matt. 14 (2002) 4177.
[13] P. Tejedor, F.E. Allegretti, P. Smilauer, B.A. Joyce, Surf. Sci. 407 (1998) 82.
[14] J. Tersoff, M.D. Johnson, B.G. Orr, Phys. Rev. Lett. 78 (1997) 282.
[15] Ch. Heyn, M. Harsdorff, Phys. Rev. B 55 (1997) 7034.
[16] M.D. Johnson, C. Orme, A.W. Hunt, D. Graff, J. Sudijono, L.M. Sander, B.G. Orr, Phys. Rev. Lett. 72 (1994) 116.
[17] C. Orme, M.D. Johnson, K.-T. Leung, B.G. Orr, P. Šmilauer, D.D. Vvedensky, J. Cryst. Growth 150 (1995) 128–135.
[18] V.R. Coluci, M.A. Cotta, C.A.C. Mendonça, K.M.I. Landers, M.M.G. de Carvalho, Phys. Rev. B 58 (1998) 1947.
[19] V.R. Coluci, M.A. Cotta, Phys. Rev. B 61 (2000) 13703.
[20] P. Šmilauer, D.D. Vvedensky, Phys. Rev. B 48 (1993) 17603.
[21] Coupled growth equations have been used earlier to describe growth on faceted surfaces. In this work, the adatom incorporation rate was dependent on the crystal facet orientation. See for example S. Koshiba, Y. Nakamura, M. Tsuchiya, H. Noge, H. Kano, Y. Nagamune, T. Noda, H. Sakaki, J. Appl. Phys. 76 (1994) 4138 or W. Braun, V.M. Kaganer, A. Trampert, H.-P. Schönherr, Q. Gong, R. Nötzel, L. Däweritz, K.H. Ploog, J. Cryst. Growth 51 (2001) 227–228.
[22] W. Braun, B. Jenichen, V.M. Kaganer, A.S. Shtukenberg, L. Däweritz, K.H. Ploog, J. Cryst. Growth 251 (2003) 56.

[23] A. Madhukar, S.V. Ghaisas, CRC Crit. Rev. Sol. State Mater. Sci. 14 (1988) 1.
[24] B.A. Joyce, J. Mater Sci. Mater Electron. 14 (2003) 591.
[25] T. Shitara, D.D. Vvedensky, M.R. Wilby, J. Zhang, J.H. Neave, B.A. Joyce, Phys. Rev. B. 46 (1992) 6825.
[26] A. Ballestad, PhD thesis, University of British Columbia, Canada. in preparation.
[27] H. Yang, V.P. LaBella, D.W. Bullock, Z. Ding, J.B. Smathers, P.M. Thibado, J. Crystal Growth 201/202 (1999) 88.
[28] P. Kratzer, E. Penev, M. Scheffler, Appl. Phys. A 75 (2002) 79.
[29] H.-C. Kan, S. Shah, T. Tadyyon-Eslami, R.J. Phaneuf, Phys. Rev. Lett. 92 (2004) 146101.